JOC The Journal of Organic Chemistry

Article

pubs.acs.org/joc

δ-Deuterium Isotope Effects as Probes for Transition-State Structures of Isoprenoid Substrates

Seoung-ryoung Choi,[†] Martin Breugst,[‡,§] Kendall N. Houk,[‡,*] and C. Dale Poulter*[,†]

[†]Department of Chemistry, University of Utah, 315 South 1400 East, Salt Lake City, Utah 84112, United States

[‡]Department of Chemistry & Biochemistry, University of California, 607 Charles E. Young Drive East, Los Angeles, California 90095, United States

Supporting Information

ABSTRACT: The biosynthetic pathways to isoprenoid compounds involve transfer of the prenyl moiety in allylic diphosphates to electron-rich (nucleophilic) acceptors. The acceptors can be many types of nucleophiles, while the allylic diphosphates only differ in the number of isoprene units and stereochemistry of the double bonds in the hydrocarbon moieties. Because of the wide range of nucleophilicities of naturally occurring acceptors, the mechanism for prenyltransfer reactions may be dissociative or associative with early to late transition states. We have measured δ-secondary kinetic isotope effects operating through four bonds for substitution reactions with dimethylallyl derivatives bearing deuterated methyl groups at the distal (C3) carbon atom in the double bond under dissociative and associative conditions. Computational studies with density functional theory indicate that the magnitudes of the isotope effects correlate with the extent of bond formation between the allylic moiety and the electron-rich acceptor in the transition state for alkylation and provide insights into the structures of the transition states for associative and dissociative alkylation reactions.

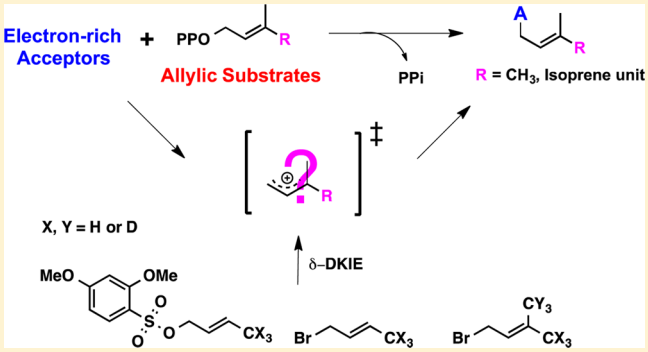

INTRODUCTION

Isoprenoid compounds form the largest and most structurally diverse family of molecules found in nature. Currently, over 60000 isoprenoid metabolites have been discovered and characterized.[1] They perform numerous important biological functions in cells, including electron transport during redox reactions (respiratory quinones), defense by plants and animals (sesquiterpenes, diterpenes, monoterpenes, isoprenoid thiols), development and reproduction (juvenile hormones, sterols, pheromones), photoprotection and vision (carotenoids), membrane structure (cholesterol, farnesylated proteins), and cell signaling (farnesylated and geranylgeranylated proteins). Isoprenoid molecules are deeply integrated into cellular function and are apparently required for life by all organisms except for a small family of highly symbiotic bacteria.[2]

Prenyltransfer reactions are the key building steps for biosynthesis of isoprenoid metabolites. They involve addition of an electrophilic allylic isoprenoid diphosphate to an electron-rich acceptor (A, see Scheme 1) with concomitant elimination of a proton and inorganic pyrophosphate (PP_i).[3−5] The allylic substrates belong to a series of isoprenoid homologues, where n = 0−4 is most common. The acceptors can be carbon−carbon double bonds, aromatic rings, hydroxyl groups, carboxylate groups, amines, and thiols/thiolates. While the allylic moiety is normally attached to the acceptor through C1 as shown in Scheme 1 (normal prenylation), attachment through C3 (reverse prenylation) is sometimes observed.[6,7] Isoprenoid cyclases catalyze intramolecular versions of the prenyltransfer reaction, where the electron-rich partner is a distal double bond in the allylic substrate.

A variety of approaches have been used to investigate the mechanisms for prenyl transfer. The most extensively studied reactions are chain elongations and cyclizations, where the electron-rich acceptor is a carbon−carbon double bond. Early on, chemists recognized that the biosynthetic reactions leading to the large variety of acyclic and cyclic isoprenoid carbon skeletons found in nature could most easily be rationalized as alkylations of carbon−carbon double bonds by allylic carbocations.[8−10] Initially, associative reactions were proposed to account for the high degree of stereoselectivity typically observed for prenyltransfer reactions,[11,12] although it is now recognized that stereoselectivity is a poor tool for distinguishing

Scheme 1. Prenyltransfer Reaction

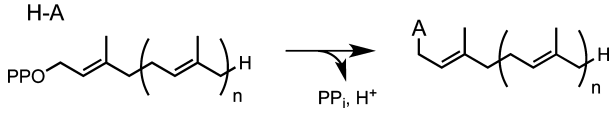

Received: February 19, 2014
Published: March 25, 2014

dx.doi.org/10.1021/jo500394u | J. Org. Chem. 2014, 79, 3572−3580

between concerted and stepwise mechanisms for enzyme-catalyzed reactions because the positions and conformations of substrates are highly ordered within an enzyme−substrate complex.

Linear free energy (LFE) correlations and product studies with alternate substrates for chain elongation prenyltransferases indicate that the reactions are dissociative.[13,14] While the LFE approach can provide important insights about mechanism, the technique requires the use of substrate analogues whose structures and binding interactions are different from those of the normal substrates. It is sometimes difficult to disentangle the effects of changing the structure of a substrate on binding and release of products from those on the chemical step. In the case of dimethylallyl tryptophan synthase, which catalyzes alkylation of the weakly nucleophilic indole nucleus in tryptophan by dimethylallyl diphosphate, LFE studies were consistent with an associative mechanism with a late transition state where substantial positive charge has developed in the dimethylallyl unit.[15] However, Tanner and co-workers recently reported secondary α-deuterium kinetic isotope effect (α-DKIE) and positional isotope exchange experiments with labeled dimethylallyl diphosphate that support a dissociative mechanism with formation of a dimethylallyl/pyrophosphate ion pair in the active site of the enzyme.[16] Protein farnesyl transferase (PFTase) catalyzes alkylation of a cysteine thiol in C-terminal four amino acid recognition motifs. Mechanistic studies suggest an associative reaction with a late transition state. Evidence for an associative process includes inversion of configuration at C1 of FPP and sensitivity to the nature of the thiolate nucleophile.[17,18] LFE studies with fluorinated analogues of FPP provide evidence for an electrophilic alkylation but do not distinguish between associative and dissociative transition states.[19] More recently, Fierke and co-workers[20] and Distefano and co-workers[21] reported primary $^{13}C-O$ and secondary α-deuterium KIEs for labeled farnesyl diphosphate that support an associative reaction with a late transition state.

The electron-rich acceptors in prenyltransfer reactions range from weakly nucleophilic carbon−carbon double bonds to powerfully nucleophilic thiolates. As the nucleophilicity of the acceptor increases, one would anticipate that the prenyltransfer reaction shifts from a dissociative to an associative mechanism with a concomitant decrease in the development of positive charge in the allylic moiety as the nucleophilicity of the acceptor increases.[22] The allylic diphosphate substrates for all prenyltransfers have a methyl group at C3, which we thought could be used as a useful probe for evaluating the structures of the transition states of the reactions. Substitution of the distal CH_3 group in (*E*)-2-chloro-3-pentene by CD_3 results in a 13% KIE during solvolysis in 95% aqueous ethanol.[23] This δ-secondary KIE is in accord with a transition state with substantial development of positive charge at the distal allylic carbon in the developing carbocation in a dissociative solvolysis reaction. In the dimethylallyl cation the magnitude of the KIE should scale with the amount of positive charge that develops at C3 in an associative reaction and approach 0 as the transition state shifts from late to early. The remote location of the isotope and the magnitude of the KIE suggest that CD_3-substituted allylic diphosphates should be excellent probes of transition state structures in prenyltransfer reactions. We now report kinetic and computational studies of δ-deuterium KIEs for allylic systems under dissociative and associative reaction conditions that confirm the predictive value of this approach.

RESULTS

Kinetic and Product Studies. *Dissociative Nucleophilic Substitution.* Secondary δ-deuterium KIEs (δ-DKIE) were determined for solvolysis of (*E*)-crotyl 2,4-dimethoxybenzenesulfonates (**1H-ODBS, 1D-ODBS**), (*E*)-crotyl bromides (**1H-Br, 1D-Br**), and 3,3-dimethylallyl bromides (**2H-Br, 2D-Br, 2D$_2$Br**) in ionizing solvents under dissociative conditions (Figure 1). Rates were measured in triplicate by monitoring

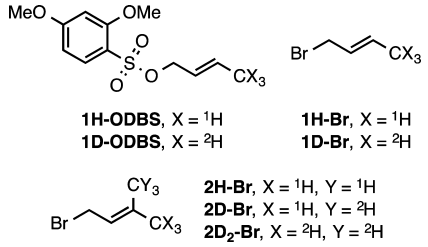

Figure 1. Allylic dimethoxybenzenesulfonates and bromides.

changes in UV absorbance for the dimethoxybenzenesulfonates and in conductivity for the bromides. First-order rate constants were determined by fitting the data to a simple exponential decay, $A = A_0e^{-kt}$, where A is UV absorbance or conductivity, t is time (seconds), and k is the first-order rate constant. The kinetic data are summarized in Table 1.

An average δ-DKIE of 1.127 was determined for solvolysis of **1H/D-ODBS** in six different solvents. These results are consistent with an increase in hyperconjugation of the methyl hydrogens with the π system as positive charge develops at C3 in the transition state for heterolysis of the C1−leaving group bond. In contrast δ-DKIE = 1.055 was determined for solvolysis of (*E*)-crotyl bromide in 80/20 H_2O/acetonitrile (v/v). Thus, the magnitude of the isotope effect decreased by 57% when the dimethoxybenzenesulfonyl leaving group in **1-ODBS** was replaced by bromide. Average δ-DKIEs of 1.081 for **2H/D-Br** and 1.206 for **2H/D$_2$-Br** were determined in five different solvents. Small variations were seen for the KIEs measured in different highly ionizing solvents.

Associative Nucleophilic Substitution. δ-DKIEs were determined for nucleophilic substitution with **1H/D-ODBS** and tetraethylammonium cyanide in DMF. Rates were measured under pseudo-first-order conditions at fixed concentrations of **1H/D-ODBS** and different concentrations of cyanide. Values for the pseudo-first-order rate constants are given in Table 2. The average δ-DKIE for k_{obs} determined at six different cyanide concentrations was 1.013. Second-order rate constants $k^H_{CN} = (7.32 \pm 0.05) \times 10^{-2}$ M^{-1} s^{-1} and $k^D_{CN} = (7.23 \pm 0.05) \times 10^{-2}$ M^{-1} s^{-1} were determined from the slopes of plots of k_{obs} versus $[CN^-]$ according to eq 1. Values for the y intercepts (k^H_0 and k^D_0) were essentially zero, as expected for a strongly associative reaction.

$$k_{obs} = k_0 + k_{CN}[CN^-] \quad (1)$$

A single substitution product, (*E*)-pent-3-enenitrile, indicated that nucleophilic attack by CN^- occurred at C1.

Computational Studies. In order to understand the observed isotope effects, density functional theory calculations were conducted employing three different dispersion-corrected functionals, B3LYP-D2,[24−26] M06-2X,[27] and ωB97X-D.[28] As solvent mixtures cannot be adequately modeled with Gaussian09, we used the major component of the mixtures,

dx.doi.org/10.1021/jo500394u | J. Org. Chem. 2014, 79, 3572−3580

Table 1. Secondary δ-Deuterium Isotope Effects for Dissociative Solvolysis of Allylic Derivatives

substrate	solvent[a]	T (°C)	k_H (10^{-3} s^{-1})	k_D (10^{-3} s^{-1})	k_H/k_D[b]
1H/D-ODBS	30W70AN	22.5	2.011 ± 0.095	1.794 ± 0.072	1.121 ± 0.011
	40W60AN	22.5	4.569 ± 0.179	4.015 ± 0.137	1.138 ± 0.010
	50W50AN	22.5	14.22 ± 0.30	12.96 ± 0.03	1.097 ± 0.006
	TFE	22.5	6.384 ± 0.368	5.573 ± 0.286	1.146 ± 0.007
	5W95TFE	22.5	7.184 ± 0.386	6.432 ± 0.354	1.117 ± 0.007
	20W80ET	22.5	2.186 ± 0.196	1.914 ± 0.204	1.142 ± 0.010
1H/D-Br	80W20AN	25	1.651 ± 0.012	1.566 ± 0.006	1.055 ± 0.003
2H/D-Br	30W70AN	25	15.39 ± 0.29	14.21 ± 0.01	1.084 ± 0.007
	40W60AN	25	72.39 ± 1.37	65.93 ± 0.73	1.098 ± 0.008
	30W70ET	25	17.59 ± 0.02	16.22 ± 0.10	1.084 ± 0.002
	5W95TFE	25	39.88 ± 0.66	37.06 ± 0.38	1.076 ± 0.007
	30W70TFE	10	35.01 ± 0.59	32.98 ± 0.12	1.061 ± 0.006
2H/D_2-Br	30W70AN	25	15.39 ± 0.29	12.77 ± 0.03	1.205 ± 0.008
	40W60AN	25	72.39 ± 1.37	57.68 ± 0.63	1.255 ± 0.009
	30W70ET	25	17.59 ± 0.02	14.85 ± 0.22	1.185 ± 0.006
	5W95TFE	25	3.88 ± 0.66	33.43 ± 0.20	1.193 ± 0.007
	30W70TFE	10	35.01 ± 0.59	29.42 ± 0.20	1.190 ± 0.007

[a]Abbreviations: AN, acetonitrile; W, water, ET, ethanol; TFE: 2,2,2-trifluoroethanol. [b]Errors were propagated from standard deviations for the rate constants according to ref 64.

Table 2. Pseudo-First-Order Rate Constants for Associative Reactions of 1H/D-ODBS in DMF at 22.5 °C

Et_4NCN (mM)	k^H_{obs} (10^{-3} s^{-1})	k^D_{obs} (10^{-3} s^{-1})	k_H/k_D
100	6.579 ± 0.123	6.607 ± 0.105	0.996 ± 0.004
120	8.654 ± 0.103	8.519 ± 0.104	1.016 ± 0.003
140	9.724 ± 0.216	9.673 ± 0.161	1.005 ± 0.005
160	11.29 ± 0.22	10.90 ± 0.27	1.036 ± 0.005
180	12.86 ± 0.07	12.56 ± 0.21	1.023 ± 0.003
240	17.01 ± 0.09	16.92 ± 0.06	1.005 ± 0.003
			1.013 ± 0.004 (av)

i.e., acetonitrile and dimethylformamide for the S_N2-type reactions and acetonitrile, ethanol, and trifluoroethanol as well as water for the S_N1-type reactions, for these calculations.

Regardless of the computational method employed, almost identical isotope effects have been calculated in all cases. The same isotope effects were calculated from scaled and unscaled harmonic frequencies, and (for S_N2 reactions) they were identical within rounding errors with those determined with the QUIVER program.[29] The Bell tunneling correction predicts that tunneling is not important for these transformations, all of which involve only secondary isotope effects. Additionally, variation of the solvent ($26.7 < \varepsilon < 78.4$) resulted in the same barriers and isotope effects. For the sake of clarity, we only discuss values obtained with B3LYP-D2 in the following, as those numbers were closest to the experimental data (see the Supporting Information for other data).

Dissociative Nucleophilic Substitution. To better understand the experimentally observed kinetic isotope effects, we investigated the dissociation reactions of **1H-ODBS**, **1H-Br**, and **2H-Br** computationally (Scheme 2). The dissociations were calculated to be endergonic (21.8 kcal mol^{-1} for **1H-ODBS**, 25.8 kcal mol^{-1} for **1H-Br**, and 19.7 kcal mol^{-1} for **2H-Br** in pure acetonitrile). While the 4 kcal mol^{-1} difference between the crotyl sulfonate (**1H-ODBS**) and bromide (**1H-Br**) can be attributed to the better stabilization of the negative

Scheme 2. Dissociative Nucleophilic Substitution of 1H/D-ODBS, 1H/D-Br, and 2H/D/D_2-Br

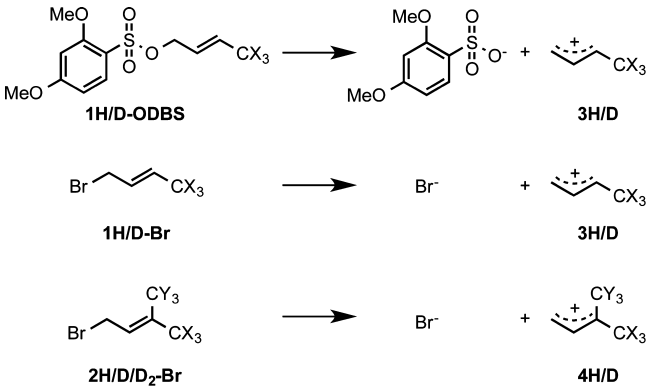

charge in the sulfonate anion in comparison to bromide, the smaller endergonicity for the dissociation of **3H** can be rationalized by the greater stability of the dimethylallyl cation **4H** in comparison to the crotyl analogue **3H**.

In general, the calculated bond lengths within the allyl cations **3H** and **4H** were very similar. The slightly elongated C−H bonds within the methyl groups (1.103 vs 1.090 for **3H** and 1.106 vs 1.093 for **4H**; see Figure S27 in the Supporting Information) reflect the stabilization of the allyl cations via hyperconjugation. According to a natural population analysis, the overall stabilizing contribution arising from all C−H−π* interactions in the dimethylallyl cation **4H** is twice the value found for the crotyl cation **3H** (**4H**, 40 kcal mol^{-1}; **3H**, 21 kcal mol^{-1}).

Additionally, we calculated the charge distribution within the allyl cations **3H** and **4H** with a variety of methods (ChelpG, Merz−Singh−Kollman, Hirshfeld, natural bond order (NBO), and atoms in molecules (AIM); see the Supporting Information for all numbers) as well as an electrostatic potential (Figure 2). While the absolute values deviate, all methods employed in this

dx.doi.org/10.1021/jo500394u | J. Org. Chem. 2014, 79, 3572−3580

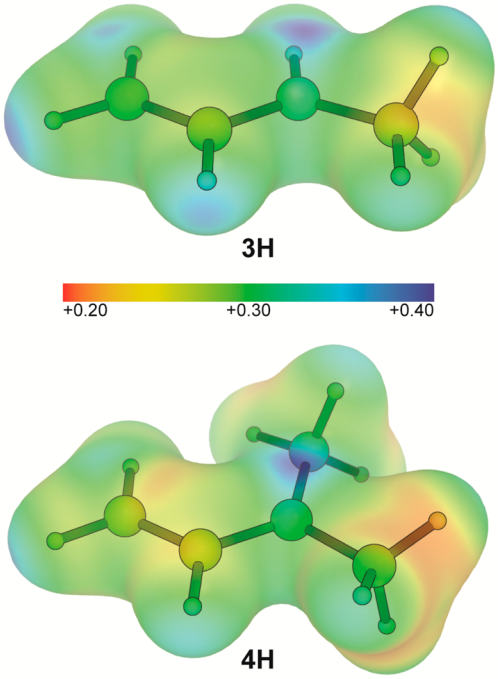

Figure 2. Calculated electrostatic potentials for the cations **3H** and **4H** (B3LYP-D2/6-31+G(d,p)/IEFPCM(acetonitrile)).

study show that a large positive charge is located on the carbon atoms 1 and 3 in both allyl cations **3H** and **4H**. The calculated electrostatic potential as well as charges calculated with the ChelpG and Merz–Singh–Kollman formalism reveal that a larger positive charge is present at the C-3 atom for both cations. Both the optimized geometries and the charges are consistent with the predominance of resonance structures with the positive charge located on the more substituted allylic terminus.

Regardless of the type of computation employed, no S_N1-type transition states could be located on the potential energy surfaces for the C–O/Br bond cleavages in **1H-ODBS, 1H-Br**, and **2H-Br**. Relaxed potential energy surface scans resulted in barrierless combinations of the sulfonates or bromides and the allylic cations in all cases, which can be attributed to the high electrophilicities of the allylic cations **3H** and **4H**.[30,31] As the dissociation of **1H-ODBS, 1H-Br**, and **2H-Br** should occur with very late transition states according to the Leffler–Hammond postulate,[32,33] the free allylic cations **3H** and **4H** were considered as transition state analogues. The calculated reaction free energy (ΔG = 21.8 kcal mol^{-1} in pure acetonitrile) for the dissociation of the crotyl sulfonate **1H-ODBS** is almost identical with the experimental activation free energy (k_1 = 2.01 × 10^{-3} s^{-1}; $\Delta G^{\ddagger}$ = 21.1 kcal mol^{-1} in 30% aqueous acetonitrile). The same agreement is also found for prenyl bromide (**2H-Br**). In contrast, the reaction free energy for the dissociation of crotyl bromide (**1H-Br**) was calculated to be slightly higher ($\Delta G^{\ddagger}$ = 23.8 kcal mol^{-1} in pure water) in comparison to the experimental value ($\Delta G^{\ddagger}$ = 21.3 kcal mol^{-1} in 80% aqueous acetonitrile), which could indicate a partial S_N2 contribution in these reactions. However, in all cases, the calculated equilibrium isotope effects should constitute an upper limit for the kinetic isotope effects determined experimentally.

The equilibrium isotope effects calculated from the free crotyl cation **3H** and the experimentally determined kinetic isotope effects for the dissociative nucleophilic substitution of crotyl sulfonates (**1H/D-ODBS**) are compared in Table 3.

Table 3. Calculated Equilibrium Isotope Effects for the Dissociation of 1H/D-ODBS[a]

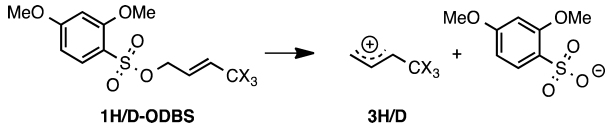

Solvent	K_H/K_D (calcd)	k_H/k_D (exptl)
acetonitrile	1.18	1.121 ± 0.011[b]
ethanol	1.18	1.142 ± 0.010[c]
TFE	1.18	1.146 ± 0.007
water	1.19	

[a]B3LYP-D2/6-31+G(d,p)/IEFPCM, various solvents, 25 °C. [b]In 30W70AN. [c]In 20W80ET.

Both values are in qualitative agreement and reflect the change in hybridization and hyperconjugation of the cation occurring in the reactions. The slight overestimation of the isotope effects can be rationalized by the fact that the transition state for the dissociation is close to but not identical with the free crotyl cation.

Tables 4 and 5 summarize the calculated equilibrium isotope effects and the experimentally determined δ-DKIEs for the

Table 4. Calculated Equilibrium Isotope Effects for the Dissociation of 1H/D-Br[a]

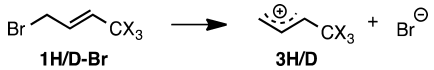

solvent	K_H/K_D (calcd)	k_H/k_D (exptl)
acetonitrile	1.17	
water	1.17	1.055 ± 0.003[b]

[a]B3LYP-D2/6-31+G(d,p)/IEFPCM, various solvents, 25 °C. [b]In 80W20AN.

Table 5. Calculated Equilibrium Isotope Effects for the Dissociation of 2H/D/D_2-Br[a]

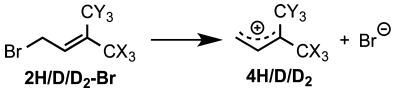

	K_H/K_D (calcd)		k_H/k_D (exptl)	
solvent	2D-Br	$2D_2$-Br	2D-Br	$2D_2$-Br
acetonitrile	1.12	1.26	1.084 ± 0.007[b]	1.205 ± 0.008[b]
trifluoroethanol	1.13	1.27	1.076 ± 0.007[c]	1.193 ± 0.007[c]
ethanol	1.14	1.28	1.084 ± 0.002[d]	1.185 ± 0.006[d]
water	1.13	1.28		

[a]B3LYP-D2/6-31+G(d,p)/IEFPCM, various solvents, 25 °C. [b]In 30W70AN. [c]In 5W95TFE. [d]In 30W70ET.

dissociative nucleophilic substitution of the crotyl and dimethylallyl bromides. Similar equilibrium isotope effects have been calculated for crotyl bromide (Table 4) and crotyl sulfonate (Table 3), while slightly smaller values have been obtained for dimethylallyl bromide. The experimentally determined kinetic isotope effect for **1H/D-Br** is only 32% of that for the corresponding sulfonate, indicating that the free allylic cation is no longer a good approximation for the bromide

dx.doi.org/10.1021/jo500394u | J. Org. Chem. 2014, 79, 3572–3580

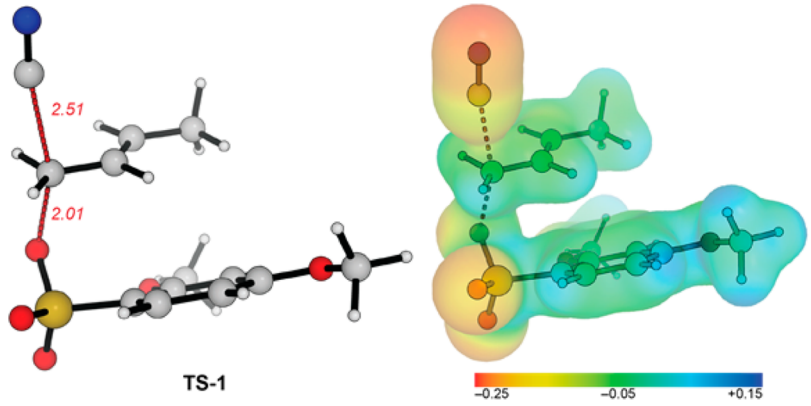

Figure 3. Calculated transition state, selected bond lengths (in Å), and calculated electrostatic potential for the S_N2 reaction of cyanide and **1H-ODBS** [B3LYP-D2/6-31+G(d,p)/IEFPCM(DMF), 25 °C].

transition state. Differences between experimental and calculated KIEs for **2H/D-Br** and **2H/D_2-Br** of approximately 63% and 72%, respectively, reflect a later transition state for dissociation of the dimethylallyl bromides.

Associative Nucleophilic Substitution. The associative nucleophilic substitution of dimethoxybenzenesulfonate by cyanide proceeds through the typical S_N2-type transition state **TS-1** (Figure 3). In the transition state, the cleaving C−O and the forming C−C bond lengths were found to be 2.01 and 2.51 Å, respectively. The calculated charge distribution (see the Supporting Information for details) as well as the electrostatic potential predicts that the negative charge is mainly located on both the sulfonate and the cyanide (ChelpG: −0.68 and −0.74, respectively), while a positive charge remains on the butenyl system (ChelpG: +0.42). These findings are in perfect agreement with the S_N2-type transition state for that reaction. For the pentavalent carbon atom, a partial charge of +0.27 has been calculated, which is significantly smaller than the partial charges for the reactive carbon atoms in the allylic cations **3H** and **4H** (**3H**, +0.38; **4H**, +0.35; see Tables S1 and S2 in the Supporting Information).

The calculated free energy of activation ($\Delta G^{\ddagger}$ = 18.8 kcal mol^{-1}) for the associative nucleophilic substitution of dimethoxybenzenesulfonate by cyanide is in excellent agreement with the experimentally determined second-order rate constant in dimethylformamide (k^{H}_{CN} = 7.32 × 10^{-2} L mol^{-1} s^{-1}, $\Delta G^{\ddagger}$ = 19.0 kcal mol^{-1}). Very small normal δ-DKIEs were calculated for the substitution reaction in both dimethylformamide and acetonitrile (Table 6). These results are in perfect agreement with the experimental observations and reflect the long distance between the reaction center and the place of isotopic exchange.

Table 6. Calculated Kinetic Isotope Effects for the S_N2 Reaction of Cyanide and 1H/D-ODBS[a]

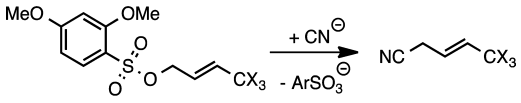

1H/D-ODBS

solvent	k_H/k_D (calcd)	k_H/k_D (exptl)
acetonitrile	1.01	
dimethylformamide	1.01	1.013 ± 0.004

[a]B3LYP-D2/6-31+G(d,p)/IEFPCM, various solvents, 25 °C.

DISCUSSION

Structures of transition states for enzyme-catalyzed reactions can provide important clues for the rational design of potent inhibitors.[34] Kinetic isotope effects give information about the reorganization of bonds as substrates are transformed into products and, in combination with ab initio computations, provide estimates of charge densities and bond lengths at the transition state. Typically, KIE experiments measure primary (bond breaking) and α-secondary (bond bending), or β-secondary (hyperconjugation) effects. In 1968, Jewett and Dunlop[23] observed an unusually large 13% δ-DKIE for solvolysis of (*E*)-2-chloro-3-pentene, where the heavy isotope was separated from the reaction center by four bonds. They attributed the KIE to hyperconjugation of developing positive charge at C3 with hydrogen/deuterium atoms in the attached methyl group. For electrophilic reactions, their results suggest that a maximal δ-DKIE will be observed for a dissociative reaction, which proceeds through a carbocationic intermediate, and a minimal value, for an associative reaction with an early transition state.

We measured δ-DKIEs for dissociative and associative displacement reactions of (*E*)-crotyl and dimethylallyl derivatives (see Table 1). The dissociative reactions exhibited simple first-order kinetic behavior, and the associative reactions showed simple pseudo-first-order behavior when run in a large excess of added nucleophile. Replacing a single CD_3 group at C3 gave δ-DKIEs from 5.5% to 14.7% for (*E*)-crotyl and dimethylallyl derivatives. In contrast, the δ-DKIE for nucleophilic substitution of (*E*)-crotyl dimethoxybenzenesulfonate by cynanide in DMF was ∼1%. These observations are consistent with the original proposal by Jewett and Dunlap[23] that the δ-DKIE arises from hyperconjugation between the methyl hydrogens and the electron-deficient allylic carbon at C3. In addition, the inverse β-DKIE for the solvolysis of 3-methyl- and 3-deuteriomethyl-4-chloro-2-pentene supports positive charge accumulations at the terminal carbon atoms of the allylic system in the transition state.[35] Density functional theory calculations indicated substantial stabilization of carbocations **3** and **4** from hyperconjugation with the methyl groups at C3, with contributions from C−H−π* for the dimethylallyl cation **4** being twice those for the crotyl cation **3**. Correspondingly, the δ-DKIEs measured for $(CD_3)_2$-dimethylallyl bromide were ∼twice those for (*E*)-CD_3-dimethylallyl bromide.

dx.doi.org/10.1021/jo500394u | J. Org. Chem. 2014, 79, 3572−3580

Relaxed potential energy surface scans gave barrierless combinations of the sulfonates or bromides with the highly electrophilic allylic cations. Since the dissociative substitutions should occur with very late transition states, the free cations **3** and **4** were considered as transition state analogues in the computational studies. Thus, the calculated δ-DKIEs should be upper limits for the experimental values. We found the experimental δ-DKIEs for the solvolysis reactions were lower than the calculated values and appeared to correlate with structural changes expected for an earlier transition state due to a nucleophilic component from solvent.[33,36] For example, experimental δ-DKIEs for **1H/D-ODBS** (for example, k_H/k_D = 1.097 in 50W50AN) were ~65% of the calculated values, while the isotope effect for **1H/D-Br** (k_H/k_D = 1.055 in 80W20AN) with a poorer leaving group was only 35% of the calculated value. In contrast, experimental δ-DKIEs for dimethylallyl bromide were substantially higher than those for crotyl bromide and the differences between experimental and computed δ-DKIEs were smaller for the dimethylallyl system.

The δ-DKIE, k_H/k_D = 1.013, measured for nucleophilic substitution of **1H/D-ODBS** by cyanide under pseudo-first-order conditions, was in excellent agreement with the isotope effect determined by computation. The very small values for k_0 relative to k_{CN} for unlabeled and labeled substrates indicate that the reaction is highly associative. A partial charge of +0.08 at C3 calculated for the associative transition state is substantially smaller than value of +0.45 computed for C3 in carbocation **3**.

There are many instances where computational tools have been used to determine structures of transition states and the underlying mechanisms for nucleophilic substitution reactions from primary and secondary kinetic isotope effects.[37−41] Notable exceptions are those based on α-DKIEs.[42−45] There is no simple linear correlation between α-DKIEs and structures of different transition states because of variations in the relative contributions from C−H/D stretching and bending modes when the reaction center is changing hybridization. In contrast, the proposed origin of the δ-DKIEs we observed involves differences in hyperconjugation that reflect changes in charge density at the distal allylic carbon, where the tetrahedral character of the directly attached CH_3/CD_3 group is basically unaltered during the substitution reaction.

CONCLUSIONS

Our studies indicate that δ-DKIEs provide an excellent tool for studying the transition state structures of prenyltransfer reactions. One anticipates that these transition states depend to a significant extent on the strength of the nucleophile in the nearby acceptor substrate, which can range from weakly nucleophilic carbon−carbon double bonds to powerfully nucleophilic thiolates. δ-DKIE measurements with deuterium-labeled substrates, along with an ab initio analysis of the data, should provide important information about bonding in the transition state. Since the magnitude of the isotope depends on the number of δ-deuterium atoms, using allylic substrates that are perdeuterated in these positions can enhance the sensitivity of the method.

EXPERIMENTAL SECTION

(*E*)-But-2-en-1-yl 2,4-Dimethoxybenzenesulfonate (1H-ODBS). To a solution of KH (60% in oil, 2.4 mmol, washed with *n*-hexane) in THF (10 mL) was added (*E*)-crotyl alcohol (2.00 mmol, 144 mg) in THF (2 mL) dropwise at −78 °C. After evolution of H_2 ceased, a solution of 2,4-methoxybenzenesulfonyl chloride (2 mmol, 472 mg) in THF (5 mL) was added dropwise at −78 °C. The mixture was stirred at −78 °C for 2 days and quenched by ice-cold saturated $NaHCO_3$. The mixture was extracted with cold ether and the extract washed with cold brine. The combined organic layers were dried over $MgSO_4$ and carefully concentrated in vacuo. Purification by flash column chromatography (silica gel, ether) gave the sulfonate ester as a colorless oil (311 mg, 63%), which was stored in ethyl ether at −78 °C until used: ^{1}H NMR (300 MHz, $CDCl_3$) δ 7.82 (d, J = 9 Hz, 1H), 6.52 (m, 2H), 5.74 (m, 1H), 5.51 (m, 1H), 4.51 (dd, J = 6.0, J = 0.9 Hz, 2H), 3.90 (s, 3H), 3.84 (s, 3H), 1.65 (dd, J = 6.0, J = 0.9 Hz, 3H); ^{13}C NMR ($CDCl_3$) 165.8, 159.2, 133.6, 133.3, 123.9, 116.8, 104.5, 99.6, 71.6, 56.4, 56.0, 17.9; HRMS (M + Na) calcd for $C_{12}H_{16}O_5SNa$ 295.0616, found 295.0623.

***tert*-Butyldiphenyl(prop-2-yn-1-yloxy)silane (4-OTBDPS).**[46,47] A solution of propargyl alcohol (1.79 g, 32.0 mmol) in CH_2Cl_2 (10 mL) was added to a solution of TBDPSCl (9.68 g, 35.2 mmol) and imidazole (2.39 g, 35.2 mmol) in CH_2Cl_2 (30 mL) at room temperature. The mixture was stirred for 5 h and diluted with ether and extracted with ether, and the extract was washed with brine, dried over $MgSO_4$, filtered, and concentrated in vacuo. The resulting crude solid was purified by flash column chromatography (95/5 hexane/ethyl acetate) to give 9.48 g (100%) of a colorless oil: ^{1}H NMR (300 MHz, $CDCl_3$) δ 7.78 (m, 4H), 7.42 (m, 6H), 4.35 (s, 2H), 2.4 (t, 1H), 1.09 (s, 9H); ^{13}C NMR ($CDCl_3$) 135.8, 133.1, 130.1, 128.0, 82.2, 73.2, 52.7, 26.9, 19.4; LCMS (M + Na) calcd for $C_{19}H_{22}OSiNa$ 317.46, found 317.1.

[$^2H_3$]Methyl *p*-Toluenesulfonate (3).[48] To a solution of *p*-toluenesulfonyl chloride (26.4 g, 0.138 mol) in THF (100 mL) were added CD_3OD (10 g, 0.277 mol) and 20% NaOH (70 mL) at °C. After 4 h, the mixture was diluted with water and extracted with ether. The combined organic layers were washed with saturated aqueous NH_4Cl and brine. The organic layer was dried over $MgSO_4$, filtered, and concentrated in vacuo to give 23.7 g (91%) of a colorless residue, which was stored at −78 °C until used: ^{1}H NMR (300 MHz, $CDCl_3$): δ 7.76 (d, J = 6 Hz, 2H), 7.33 (d, J = 6 Hz, 2H), 2.42 (s, 3H); ^{13}C NMR 145.1, 132.3, 130.2, 128.2, 21.8.

([4-$^2H_3$]2-Butyn-1-yloxy)*tert*-butyldiphenylsilane (5D-OTBDPS).[47] To a solution of **4-OTBDPS** (6.51 g, 22.1 mmol) in THF (40 mL) was slowly added n-BuLi (10.6 mL, 26.5 mmol, 2.5 M solution in hexane) at 0 °C. After 10 min, [$^2H_3$]methyl tosylate **3** (5.02 g, 26.5 mmol) was slowly added and the resulting mixture was stirred at room temperature overnight. The mixture was diluted with ethyl acetate and washed with saturated aqueous NH_4Cl solution and brine. The organic layer was dried over $MgSO_4$ and concentrated under vacuum. The residue was purified by flash column chromatography on silica gel (10/1 hexane/ether) to give 6.4 g (93%) of a pale yellow oil: ^{1}H NMR (300 MHz, $CDCl_3$) δ 7.78 (m, 4H), 7.4 (m, 6H), 4.34 (s, 2H), 1.09 (s, 9H); ^{13}C NMR ($CDCl_3$) 135.8, 133.5, 129.9, 127.9, 81.4, 77.8, 53.1, 26.9, 19.4; LCMS (M + Na) calcd $C_{20}H_{21}D_3OSiNa$ 334.5, found 334.1.

[4-$^2H_3$]But-2-yn-1-ol (5D-OH).[47,49] To a solution of **5D-OTBDPS** (6.4 g, 20.6 mmol) in THF (100 mL) was added TBAF hydrate (16.1 g, 61.7 mmol) at room temperature. The mixture was stirred for 4.5 h, diluted with water, and extracted with ether. The combined organic layers were washed with brine and dried over Mg_2SO_4. Solvent was carefully removed under vacuum. The residue was purified by flash column chromatography on silica gel (2/1 pentane/diethyl ether) to give 727 mg (78%) of a colorless liquid: ^{1}H NMR (300 MHz, $CDCl_3$) δ 4.21 (s, 2H), 1.53 (s, OH); ^{13}C NMR ($CDCl_3$) 81.6, 77.8, 50.8 (deuterated C4 was not detected); GCMS (m/z, $[M - H]^+$) calcd $C_4H_2D_3O$ 72.05, found 72.08; GCMS (m/z, $[M - OH]^+$) calcd for $C_4H_2D_3$ 56.06, found 56.10.

(*E*)-[4-$^2H_3$]2-Buten-1-ol (1D-OH).[47] To a suspension of lithium aluminum hydride (95%, 350 mg, 9.2 mmol) in dry THF (20 mL) was slowly added deuterated butynol **5D-OH** (518 mg, 7 mmol) in dry THF (5 mL) at 0 °C. The ice bath was removed, and the reaction mixture was stirred at room temperature for 22 h. The reaction was quenched by the sequential addition of water (1 mL), 30% NaOH (1 mL), and water (1 mL). The resulting suspension was filtered and washed with diethyl ether. The ether layer was dried over $MgSO_4$. The

dx.doi.org/10.1021/jo500394u | J. Org. Chem. 2014, 79, 3572−3580

solvent was removed through a distilling column. Distillation of the residue gave 208 mg (40%) of a colorless liquid: ^{1}H NMR (300 MHz, $CDCl_3$) δ 5.65 (m, CH═CH), 4.05 (d, J = 4.8 Hz, 2H); ^{13}C NMR ($CDCl_3$) 130.4, 128.1, 63.8 (deuterated C4 was not detected); GCMS (m/z) calcd for $C_4H_5D_3O$ 75.08, found 74.9.

(*E*)-[4-$^2H_3$]But-2-en-1-yl 2,4-Dimethoxybenzenesulfonate (1D-ODBS). The colorless oil (218 mg, 63%) was synthesized as described above for **1H-ODBS**: ^{1}H NMR (300 MHz, $CDCl_3$) δ 7.8 (d, J = 9 Hz, 1H), 6.5 (m, 2H), 5.7 (m, 1H), 5.29 (m, 1H), 4.5 (dd, J = 6.6, J = 1.2, 2H), 3.9 (s, 3H), 3.84 (s, 3H); ^{13}C NMR ($CDCl_3$) 165.7, 159.2, 133.5, 133.3, 123.9, 116.8, 104.4, 99.6, 71.6, 56.4, 55.9; HRMS (M+Na): calcd for $C_{12}H_{13}D_3O_5SNa$ 298.0804, found 298.0801.

(*E*)-1-Bromo-2-butene (1H-Br).[50] To a solution of (*E*)-crotyl alchol (721 mg, 10 mmol) in dry ether (25 mL) was added PBr_3 (0.47 mL, 5 mmol) via a syringe at 0 °C. The mixture was stirred for 30 min at 0 °C and for additional 30 min at room temperature. Ice was added to quench the reaction. The ether layer was washed with brine, dried over $MgSO_4$ and evaporated. The crude residue was purified by a vacuum distillation (50 mmHg) at rt (bp lit. 97−99 °C[50]) to afford a colorless oil (0.76 g, 90%); ^{1}H NMR (300 MHz, $CDCl_3$) δ 5.74 (m, 2H), 3.93 (ddq, J = 0.6, J = 3.6, J = 6.6 Hz, 2H), 1.72 (ddt, J = 0.9, J = 1.8, J = 5.7 Hz, 3H); ^{13}C NMR ($CDCl_3$) 131.5, 127.7, 33.7, 17.8; GCMS (m/z): calcd for C_4H_7Br 133.97, found 134.06.

(*E*)-[4-$^2H_3$]-1-Bromo-2-butene (1D-Br). To a solution of (*E*)-butenol **1D-OH** (0.6 g, 7.98 mmol) in dry ether (5 mL) was added PBr_3 (0.38 mL, 3.99 mmol) via a syringe at 0 °C. The mixture was stirred for 30 min at 0 °C and for an additional 30 min at room temperature. Ice was added to quench the reaction. The ether layer was washed with brine, dried over $MgSO_4$, and evaporated. The crude residue was purified by vacuum distillation to afford a colorless oil (0.66 g, 60%): ^{1}H NMR (300 MHz, $CDCl_3$) δ 5.72 (m, 2H), 3.94 (d, J = 6.6 Hz, 2H); ^{13}C NMR ($CDCl_3$) 131.5, 127.8, 33.7; GCMS (m/z) calcd for $C_4H_4D_3Br$ 136.99, found 137.1.

(*Z*)-3-Iodo-2-butenol (6-OH).[51] To a solution of 2-butyn-1-ol (5.8 g, 82.7 mmol) in 90 mL of ether was added dropwise Red-Al (41.8 mL, 124 mmol, 60 wt % in toluene) at −78 °C. The reaction mixture was warmed to room temperature and stirred overnight. The reaction mixture was cooled to −78 °C and quenched with a solution of I_2 (63 g, 248 mmol) in THF (200 mL). The mixture was warmed to room temperature and stirred for 2 h. Saturated aqueous $Na_2S_2O_3$ was added to the mixture, and the layers were separated. The aqueous layer was extracted with ether (×3), and the combined ether layers were washed with brine, dried over $MgSO_4$, and evaporated. The crude product was purified by flash column chromatography (2/3 ethyl acetate/hexane) to give a light yellow oil (12.9 g, 78.8%): ^{1}H NMR (300 MHz, $CDCl_3$) δ 5.68 (tq, J = 5.85, J = 1.5, 1H), 4.06 (dq, J = 5.85, J = 1.2, 2H), 3.46 (s, OH), 2.48 (dd, J = 2.85, J = 1.5, 3H); ^{13}C NMR ($CDCl_3$) 134.5, 101.8, 67.4, 33.9; GCMS (m/z) calcd for C_4H_7IO 197.95, found 198.0.

(*Z*)-*tert*-Butyl((3-iodobut-2-en-1-yl)oxy)diphenylsilane (6-OTBDPS). The protection was performed as described in the synthesis of **4-OTBDPS**. Butenol **6-OH** (4.2 g, 21.2 mmol) in CH_2Cl_2 (20 mL) was added to a solution of TBDPSCl (6.99 g, 25.4 mmol) and imidazole (1.73 g, 25.4 mmol) in CH_2Cl_2 (50 mL) at room temperature. The resulting crude product was purified by flash column chromatography (12/1 hexane/ethyl acetate) to give 8.9 g (96.2%) of a colorless oil: ^{1}H NMR (300 MHz, $CDCl_3$) δ 7.72 (m, 4H), 7.42 (m, 6H), 5.81 (tq, J = 5.4, J = 1.5 Hz, 1H), 4.26 (dq, J = 5.4, J = 1.5 Hz, 2H), 2.50 (dd, J = 3.0, J = 1.5 Hz, 3H), 1.09 (s, 9H); ^{13}C NMR ($CDCl_3$) 135.8, 135.2, 133.7, 129.9, 127.9, 99.4, 69.4, 33.7, 27.0, 19.4; GCMS (m/z, [M − C_4H_9]$^+$) calcd for $C_{16}H_{16}IOSi$ 379.00, found 379.1.

(*Z*)-[4′-$^2H_3$]-*tert*-Butyl((3-methylbut-2-en-1-yl)oxy)diphenylsilane (2D-OTBDPS).[52] LiCl (30 mmol) was placed in an N_2-flushed flask and dried for 20 min at 150−170 °C under vacuum. Zinc dust (30 mmol) was added, and the heterogeneous mixture of Zn and LiCl was dried again for 20 min at 150−170 °C under vacuum. THF (5 mL) was added, and the Zn was activated with $BrCH_2CH_2Br$ (5 mol %) and TMSCl (1 mol %). A solution of CD_3I (4.35 g, 30 mmol) in THF (30 mL) was then added at room temperature. The mixture was stirred at 35−40 °C overnight. The solution of CD_3ZnI was separated from the remaining zinc dust and added to a solution of **6-OTBDPS** (6.80 g, 15.6 mmol) and $Pd(Ph_3)_4$ (1 mol %) in THF (50 mL) at room temperature. The mixture was stirred at room temperature for 6 h and quenched by adding saturated aqueous NH_4Cl. The quenched mixture was extracted with ether, and the extract was washed with brine and dried over $MgSO_4$. The crude residue was purified by column chromatography (hexane) to yield a colorless oil (4.83 g, 94.7%): ^{1}H NMR (300 MHz, $CDCl_3$) δ 7.76 (m, 4H), 7.44 (m, 6H), 5.45 (dq, J = 6.3, J = 1.5 Hz, 1H), 4.42 (dq, J = 6.4, J = 1.2 Hz, 2H), 1.75 (dd, J = 1.2 Hz, 3H), 1.12 (s, 9H); ^{13}C NMR ($CDCl_3$) 135.9, 134.3, 129.7, 127.8, 124.5, 61.4, 27.1, 25.9, 19.4; GCMS (m/z, [M − C_4H_9]$^+$) calcd for $C_{17}H_{16}D_3OSi$ 270.14, found 270.10.

(*Z*)-[4′-$^2H_3$]-3-Methyl-2-butenol (2D-OH). The deprotection was performed as described in the synthesis of **5D-OH.** To a solution of **2D-OTBDPS** (4.6 g, 14 mmol) in THF (90 mL) was added TBAF (18 mmol, 1 M in THF) at room temperature. The resulting residue was purified by flash column chromatography (3/1 pentane/ether) to yield a colorless oil (1.15 g, 92%): ^{1}H NMR (300 MHz, $CDCl_3$) δ 5.32 (tq, J = 6.0, J = 1.5 Hz, 1H), 4.03 (d, J = 7.2 Hz, 2H), 2.56 (s, OH), 1.67 (dd, J = 1.2 Hz, 3H); ^{13}C NMR ($CDCl_3$) 135.8, 123.9, 59.2, 25.8; GCMS (m/z) calcd for $C_5H_7D_3O$ 89.09, found 89.1.

(Z)-[4′-$^2H_3$]-1-Bromo-3-methyl-2-butene (2D-Br).[53] To a solution of **2D-OH** (0.59 g, 6.6 mmol) in dry ether (15 mL) was added PBr_3 (0.31 mL, 3.3 mmol) via a syringe at 0 °C. The mixture was stirred for 30 min at 0 °C and for an additional 30 min at room temperature. Ice was added to quench the reaction. The ether layer was washed with brine, dried over $MgSO_4$, and evaporated. The crude product was purified by vacuum distillation to give a colorless oil (0.66 g, 66%): ^{1}H NMR (300 MHz, $CDCl_3$) δ 5.51 (tq, J = 8.5, J = 1.5 Hz, 1H), 4.00 (dq, J = 8.7, J = 0.6 Hz, 2H), 1.76 (dt, J = 1.5, J = 0.6 Hz, 3H); ^{13}C NMR ($CDCl_3$) 140.2, 121.0, 29.9, 25.9; GCMS (m/z) calcd for $C_5H_6D_3Br$ 151.1, found 151.1.

[4,4′-$^2H_6$]-Ethyl 3-Methyl-2-butenoate (7).[54] To a solution of triethylphosphonoacetate (26.2 g, 117 mmol) in THF (200 mL) was slowly added n-BuLi (109 mmol, 2.5 M in hexane) at 0 °C. After the mixture was stirred until bubbling ceased at room temperature, acetone-d_6 (5 g, 77.98 mmol) in THF (50 mL) was added to the anion of the phosphonate. The mixture was stirred for 3 h at room temperature and quenched by adding saturated aqueous NH_4Cl. The aqueous layer was extracted with diethyl ether. The combined organic layers were washed with brine and dried over $MgSO_4$. The product was purified by flash column chromatography (2/1 pentane/ether) to give a light yellow oil (8.29 g, 79.3%): ^{1}H NMR (300 MHz, $CDCl_3$) δ 5.64 (s, 1H), 4.12 (q, J = 7.14 Hz, 2H), 1.24 (t, J = 7.14 Hz, 3H); ^{13}C NMR ($CDCl_3$) 166.8, 156.3, 116.3, 59.5, 14.4; GCMS (m/z) calcd for $C_7H_6D_6O_2$ 134.12, found 134.0.

[4,4′-$^2H_6$]-3-Methyl-2-butenol ($2D_2$-OH).[55] To a suspension of LAH (2.67 g, 70.5 mmol) in THF (100 mL) was added a solution of butenoate 7 (9.3 g, 47 mmol) in THF (30 mL) at 0 °C. The mixture was stirred at 0 °C and at room temperature for 30 min. Ether (50 mL) was added to dilute the mixture, and Na_2SO_4 (80 g) mixed with water (20 mL) was added in portions at 0 °C. After the mixture was stirred for 1 h at room temperature, additional Na_2SO_4 was added to remove water. The solid was filtered off and washed with ether. Purification by flash column chromatography (1/2 ether/pentane) afforded a colorless oil (2.73 g, 63%): ^{1}H NMR (300 MHz, $CDCl_3$) δ 5.31 (t, J = 6.9, 1H), 4.02 (d, J = 6.9 Hz, 2H), 2.73 (s, OH); ^{13}C NMR ($CDCl_3$) 135.6, 123.9, 59.1; GCMS (m/z) calcd for $C_5H_4D_6O$ 92.11, found 92.18.

[4,4′-$^2H_6$]-1-Bromo-3-methyl-2-butene ($2D_2$-Br). The bromination was performed as described in the synthesis of **2D-Br**. To a solution of **$2D_2$-OH** (0.5 g, 5.42 mmol) in dry ether (25 mL) was added PBr_3 (0.26 mL) via a syringe at 0 °C. The crude residue was purified by vacuum distillation to afford a colorless oil (0.76 g, 90%): ^{1}H NMR (300 MHz, $CDCl_3$) δ 5.50 (t, J = 8.4 Hz, 1H), 3.98 (d, J = 8.4 Hz, 2H); ^{13}C NMR ($CDCl_3$) 140.1, 121.0, 29.9; GCMS (m/z) calcd for $C_5H_3D_6Br$ 154.03, found 154.06.

Kinetic Measurements. Rates for dissociative nucleophilic substitution reactions of 2,4-dimethoxybenzenesulfonate esters (0.1

dx.doi.org/10.1021/jo500394u | J. Org. Chem. 2014, 79, 3572−3580

mM) and bromides (0.6 or 1 mM) were measured in 30/70−80/20 H_2O/AcCN (v/v), TFE, 95/5 TFE/H_2O (v/v), or 60/40−80/20 EtOH/H_2O (v/v)). Rates for associative nucleophilic substitution reactions for were measured in 100−240 mM tetraethylammonium cyanide in dry DMF. Time courses for reactions of sulfonate esters were determined from UV absorbance measured at 30 s intervals at six different wavelengths between 225 and 290 nm. Time courses for bromides were determined from changes in conductivity measured at 1 s intervals. Measurements were in triplicate at 10, 22.5, or 25 °C.

Product Studies: (*E*)-Pent-3-enenitrile. To 0.3 g (1.19 mmol) of **1** in diethyl ether (10 mL) was added tetraethylammonium cyanide (224 mg, 1.42 mmol) in acetonitrile (5 mL) at room temperature, and the progress of the reaction was monitored by TLC. Upon completion, the mixture was diluted with diethyl ether and passed through a short plug of silica gel. Solvent was removed by careful distillation to give 35 mg (36%) of a pale yellow oil: ^{1}H NMR (300 MHz, $CDCl_3$) δ 5.79 (m, 1H), 5.39 (m, 1H), 3.04 (ddt, J = 5.7, J = 3.3 Hz, J = 1.5, 2H), 1.72 (dq, J = 6.6, J = 1.5 Hz, 3H); ^{13}C NMR 131.2, 118.4, 118.1, 20.5, 17.8; GCMS (m/z) calcd 81.06, found 81.00.

Computational Methods. The conformational space of each intermediate was explored using the OPLS_2005 force field[56] and a modified Monte Carlo search routine implemented in MACROMODEL 9.9.[57] All structures were subsequently optimized employing B3LYP-D2,[24−26] M06-2X,[27] or ωB97X-D[28] with the double-ζ split-valence 6-31+G(d,p) basis set. Solvation by different solvents was taken into account using the IEFPCM continuum solvation model[58] in both optimization and frequency calculations. For solvent mixtures, the major component was chosen for the solvation model. It has recently been shown that the presence of a polarizable continuum model does not have a large impact on frequencies, while solvation is sometimes necessary to locate certain transition states that only exist in polar media.[59] Very tight convergence criteria during the geometry optimizations and an ultrafine grid for numerical integration of the density were used throughout this study. Vibrational analysis verified that each structure was a minimum or a transition state. Thermal corrections were calculated from unscaled harmonic frequencies for a standard state of 298.15 K and 1 mol L^{-1}. All computations were performed using Gaussian 09.[60] The reported isotope effects were calculated from computed free energies and were identical within rounding with values obtained from the QUIVER program (where available).[29] Tunneling in the S_N2 reactions was evaluated with the infinite parabolic model of Bell.[61−63]

■ ASSOCIATED CONTENT

Supporting Information

Text, figures, and tables giving additional experimental methods, characterization data, monitored kinetic data, and computational details. This material is available free of charge via the Internet at http://pubs.acs.org.

■ AUTHOR INFORMATION

Corresponding Authors

*E-mail for K.N.H.: houk@chem.ucla.edu.

*E-mail for C.D.P.: poulter@chem.utah.edu.

Present Address

[§]Department für Chemie, Universität zu Köln, Greinstraße 4, 50939 Köln, Germany.

Notes

The authors declare no competing financial interest.

■ ACKNOWLEDGMENTS

We are grateful to the Alexander von Humboldt Foundation (Feodor Lynen scholarship to M.B.), the National Institutes of Health (GM-21328 to C.D.P.), and the National Science Foundation (CHE-0548209 to K.N.H.) for financial support of this research. This work used the Extreme Science and Engineering Discovery Environment (XSEDE), which is supported by National Science Foundation Grant No. OCI-1053575 and resources from the UCLA Institute for Digital Research and Education (IDRE). We thank Dr. Matthew Janczak for help with error analysis.

■ REFERENCES

(1) Dictionary of Natural Products (http://dnp.chemmetbase.com).
(2) Pérez-Brocal, V.; Gil, R.; Ramos, S.; Lamelas, A.; Postigo, M.; Michelena, J. M.; Silva, F. J.; Moya, A.; Latorre, A. *Science (Washington, DC, U.S.)* **2006**, *314*, 312.
(3) Poulter, C. D. *Phytochem. Rev.* **2006**, *5*, 17.
(4) Wang, K.; Ohnuma, S.-i. *Trends Biochem. Sci.* **1999**, *24*, 445.
(5) Kellogg, B. A.; Poulter, C. D. *Curr. Opin. Chem. Biol.* **1997**, *1*, 570.
(6) Rudolf, J. D.; Wang, H.; Poulter, C. D. *J. Am. Chem. Soc.* **2013**, *135*, 1895.
(7) Thulasiram, H. V.; Erickson, H. K.; Poulter, C. D. *Science* **2007**, *316*, 73.
(8) Wendt, K. U.; Schulz, G. E. *Structure (London)* **1998**, *6*, 127.
(9) Cane, D. E. *Acc. Chem. Res.* **1985**, *18*, 220.
(10) Dolence, J. M.; Poulter, C. D. *Compr. Nat. Prod. Chem.* **1999**, *5*, 315.
(11) Cornforth, J. W.; Cornforth, R. H.; Popják, G.; Yengoyan, L. *J. Biol. Chem.* **1966**, *241*, 3970.
(12) Cornforth, J. W. *Angew. Chem., Int. Ed. Engl.* **1968**, *7*, 903.
(13) Poulter, C. D.; Wiggins, P. L.; Le, A. T. *J. Am. Chem. Soc.* **1981**, *103*, 3926.
(14) Mash, E. A.; Gurria, G. M.; Poulter, C. D. *J. Am. Chem. Soc.* **1981**, *103*, 3927.
(15) Gebler, J. C.; Woodside, A. B.; Poulter, C. D. *J. Am. Chem. Soc.* **1992**, *114*, 7354.
(16) Luk, L. Y. P.; Tanner, M. E. *J. Am. Chem. Soc.* **2009**, *131*, 13932.
(17) Mu, Y.; Omer, C. A.; Gibbs, R. A. *J. Am. Chem. Soc.* **1996**, *118*, 1817.
(18) Huang, C.-c.; Hightower, K. E.; Fierke, C. A. *Biochemistry* **2000**, *39*, 2593.
(19) Dolence, J. M.; Poulter, C. D. *Proc. Natl. Acad. Sci. U.S.A.* **1995**, *92*, 5008.
(20) Pais, J. E.; Bowers, K. E.; Fierke, C. A. *J. Am. Chem. Soc.* **2006**, *128*, 15086.
(21) Lenevich, S.; Xu, J.; Hosokawa, A.; Cramer, C. J.; Distefano, M. D. *J. Am. Chem. Soc.* **2007**, *129*, 5796.
(22) Mayr, H.; Förner, W.; Schleyer, P. v. R. *J. Am. Chem. Soc.* **1979**, *101*, 6032.
(23) Jewett, J. G.; Dunlap, R. P. *J. Am. Chem. Soc.* **1968**, *90*, 809.
(24) Becke, A. D. *J. Chem. Phys.* **1993**, *98*, 5648.
(25) Lee, C.; Yang, W.; Parr, R. G. *Phys. Rev. B* **1988**, *37*, 785.
(26) Grimme, S. *J. Comput. Chem.* **2006**, *27*, 1787.
(27) Zhao, Y.; Truhlar, D. G. *Theor. Chem. Acc.* **2008**, *120*, 215.
(28) Chai, J.-D.; Head-Gordon, M. *Phys. Chem. Chem. Phys.* **2008**, *10*, 6615.
(29) Saunders, M.; Laidig, K. E.; Wolfsberg, M. *J. Am. Chem. Soc.* **1989**, *111*, 8989.
(30) Mayr, H.; Kempf, B.; Ofial, A. R. *Acc. Chem. Res.* **2003**, *36*, 66.
(31) Troshin, K.; Schindele, C.; Mayr, H. *J. Org. Chem.* **2011**, *76*, 9391.
(32) Leffler, J. E. *Science* **1953**, *117*, 340.
(33) Hammond, G. S. *J. Am. Chem. Soc.* **1955**, *77*, 334.
(34) Schramm, V. L. *Annu. Rev. Biochem.* **2011**, *80*, 703.
(35) Griffin, R. H.; Jewett, J. G. *J. Am. Chem. Soc.* **1970**, *92*, 1104.
(36) Shiner, V. J.; Fisher, R. D. *J. Am. Chem. Soc.* **1971**, *93*, 2553.
(37) Melissas, V. S.; Truhlar, D. G. *J. Chem. Phys.* **1993**, *99*, 3542.
(38) Beno, B. R.; Houk, K. N.; Singleton, D. A. *J. Am. Chem. Soc.* **1996**, *118*, 9984.
(39) Berti, P. J.; Schramm, V. L. *J. Am. Chem. Soc.* **1997**, *119*, 12069.
(40) Singleton, D. A.; Wang, Z. *J. Am. Chem. Soc.* **2005**, *127*, 6679.
(41) Gonzalez-James, O. M.; Singleton, D. A. *J. Am. Chem. Soc.* **2010**, *132*, 6896.

(42) Fang, Y.-r.; Gao, Y.; Ryberg, P.; Eriksson, J.; Kołodziejska-Huben, M.; Dybała-Defratyka, A.; Madhavan, S.; Danielsson, R.; Paneth, P.; Matsson, O.; Westaway, K. C. *Chem. Eur. J.* **2003**, *9*, 2696.
(43) Fang, Y.-r.; MacMillar, S.; Eriksson, J.; Kołodziejska-Huben, M.; Dybała-Defratyka, A.; Paneth, P.; Matsson, O.; Westaway, K. C. *J. Org. Chem.* **2006**, *71*, 4742.
(44) Dzierzawska, J.; Jarota, A.; Karolak, M.; Piotrowski, L.; Placek, I.; Swiderek, K.; Szatkowski, L.; Paneth, P. *J. Phys. Org. Chem.* **2007**, *20*, 1114.
(45) Westaway, K. C.; Fang, Y.-r.; MacMillar, S.; Matsson, O.; Poirier, R. A.; Islam, S. M. *J. Phys. Chem. A* **2008**, *112*, 10264.
(46) Larrosa, I.; Da Silva, M. I.; Gómez, P. M.; Hannen, P.; Ko, E.; Lenger, S. R.; Linke, S. R.; White, A. J. P.; Wilton, D.; Barrett, A. G. M. *J. Am. Chem. Soc.* **2006**, *128*, 14042.
(47) Tokiwano, T.; Watanabe, H.; Seo, T.; Oikawa, H. *Chem. Commun. (Cambridge, U.K.)* **2008**, 6016.
(48) Oikawa, H.; Suzuki, Y.; Katayama, K.; Naya, A.; Sakano, C.; Ichihara, A. *J. Chem. Soc., Perkin Trans. 1* **1999**, 1225.
(49) Mohanty, S. S.; Uebelhart, P.; Eugster, C. H. *Helv. Chim. Acta* **2000**, *83*, 2036.
(50) Geiseler, O.; Podlech, J. *Tetrahedron* **2012**, *68*, 7280.
(51) Dakoji, S.; Li, D.; Agnihotri, G.; Zhou, H.-q.; Liu, H.-w. *J. Am. Chem. Soc.* **2001**, *123*, 9749.
(52) Krasovskiy, A.; Malakhov, V.; Gavryushin, A.; Knochel, P. *Angew. Chem., Int. Ed.* **2006**, *45*, 6040.
(53) Thulasiram, H. V.; Phan, R. M.; Rivera, S. B.; Poulter, C. D. *J. Org. Chem.* **2006**, *71*, 1739.
(54) Candito, D. A.; Dobrovolsky, D.; Lautens, M. *J. Am. Chem. Soc.* **2012**, *134*, 15572.
(55) Candito, D. A.; Panteleev, J.; Lautens, M. *J. Am. Chem. Soc.* **2011**, *133*, 14200.
(56) Banks, J. L.; Beard, H. S.; Cao, Y.; Cho, A. E.; Damm, W.; Farid, R.; Felts, A. K.; Halgren, T. A.; Mainz, D. T.; Maple, J. R.; Murphy, R.; Philipp, D. M.; Repasky, M. P.; Zhang, L. Y.; Berne, B. J.; Friesner, R. A.; Gallicchio, E.; Levy, R. M. *J. Comput. Chem.* **2005**, *26*, 1752.
(57) *MacroModel, version 9.9*; Schrödinger, LLC, New York, 2012.
(58) Cancès, E.; Mennucci, B.; Tomasi, J. *J. Chem. Phys.* **1997**, *107*, 3032.
(59) Ribeiro, R. F.; Marenich, A. V.; Cramer, C. J.; Truhlar, D. G. *J. Phys. Chem. B* **2011**, *115*, 14556.
(60) Frisch, M. J.; Trucks, G. W.; Fox, D. J., et al. *Gaussian 09*; Gaussian, Inc., Wallingford, CT, 2009.
(61) Bell, R. P. *Trans. Faraday Soc.* **1959**, *55*, 1.
(62) Bell, R. P. *Chem. Soc. Rev.* **1974**, *3*, 513.
(63) Bell, R. P. *The Tunnel Effect in Chemistry*; Chapman and Hall: London, 1980.
(64) Harris, D. C. *Experimental Error in Quantitative Chemical Analysis*, 5th ed.; W. H. Freeman: New York, 1999; pp 58−63.